Numerical simulation of a negative ion plasma expansion into vacuum

L. G. Garcia, J. Goedert, H. Figua, E. Fijalkow, and M. R. Feix

Citation: Physics of Plasmas **4**, 4240 (1997); doi: 10.1063/1.872587
View online: http://dx.doi.org/10.1063/1.872587
View Table of Contents: http://scitation.aip.org/content/aip/journal/pop/4/12?ver=pdfcov
Published by the AIP Publishing

Numerical simulation of a negative ion plasma expansion into vacuum

L. G. Garcia and J. Goedert
Instituto de Física, UFRGS, Caixa Postal 15051, 91500-970 Porto Alegre, RS—Brazil

H. Figua, E. Fijalkow, and M. R. Feix
Laboratoire de Mathématiques, Appliquées et Physique Mathématique d'Orlèans, Département de Mathématiques—UFR Sciences, BP 6759-45067 Orléans Cedex 2, France

(Received 8 July 1997; accepted 27 August 1997)

The expansion into vacuum of a one-dimensional, collisionless, negative ion plasma is investigated in the framework of the Vlasov–Poisson model. The basic equations are written in a ''new time space'' by use of a rescaling transformation and, subsequently, solved numerically through a fully Eulerian code. As in the case of a two species plasma, the time-asymptotic regime is found to be self-similar with the temperature decreasing as t^{-2}. The numerical results exhibit clearly the physically expected effects produced by the variation of parameters such as initial temperatures, mass ratios and charge of the negative ions. © *1997 American Institute of Physics.* [S1070-664X(97)00712-X]

I. INTRODUCTION

The subject of plasma expansion into vacuum has received significant attention over the last decades. This phenomenon has been studied not only for a two component plasma case,[1–5] but also for plasmas with three species.[6,7] In particular, the interest in the plasma expansion process can be justified by its potential application in space physics[2] and in laboratory experiments.[3,4] In these applications it is common to find a large number of negatively charged dust grains that can significantly alter the properties of the plasma. Dusty plasmas are frequently approximated by ''negative ion plasmas'' (NIP) which consist of positive ions, electrons and negative ions of constant charge. In this work we present a numerical study of the behavior of a NIP in the process of free expansion into vacuum.

Current models for describing the basic dynamics of a plasma expansion into vacuum are essentially electrostatic[5] and the majority are based on a fluid description;[7,8] nevertheless, kinetic models have also been considered.[5,8,9] In general these descriptions (kinetic and fluid) are associated with assumptions of quasineutrality and Boltzmann densities for the electrons and positive ions. El-Zein *et al.*[6] improved on the usual fluid models by considering charge separation effects through the inclusion of Poisson's equation in the fluid model. They also abandoned the hypothesis of thermal equilibrium (Boltzmann densities) for the positive ions in favor of the more realistic momentum balance and continuity equations. In the fluid model of Yu and Luo[10] the possibility of charge variation for the negative ions, as well as pressure effects, were also taken into account. However, they still assumed quasi-neutrality and Boltzmann densities for electrons and positive ions. The possibility of charge variation is an important contribution since in real dusty plasmas, as we know, the charge of the dust particles can vary according to the densities of electrons and ions and to the local electrostatic field. The main proposal of this paper is to numerically analyze the free expansion of an NIP into vacuum over long times and study how the variation in the negative ion concentration, initial temperatures and the mass ratios can affect the expansion process. For this purpose we use a one-dimensional Vlasov–Poisson model without imposing quasi-neutrality or Boltzmann densities for any of the species.

It is well established that simulations of plasma free expansion over long times run into difficulties[5] in several respects. An expansion into vacuum requires free boundary conditions and the expanding plasma requires more and more place in space as time increases. So the computational box has to increase with time to avoid having the plasma reach the boundaries, making it impossible to implement free boundary conditions. A practical way to bypass this difficulty was used by Manfredi, Mola and Feix;[5] they applied a method proposed by Burgan *et al.*[11] whereby a self-similarity transformation rescales the phase space, which then is kept of constant size by a proper choice of a parameter. In that transformed space, free boundary conditions were easily implemented. After the transformation, Manfredi *et al.* use an Eulerian code to solve numerically the Vlasov equation. The Poisson equation in one dimension, resuming in a simple differential equation, is solved by integrating a spline collocation polynomial. Contrary to the usual particle code, the Eulerian code yields good resolution of the phase space structure even in the low density regime. The same strategy will be applied in this paper to the free expansion of an NIP into vacuum.

In our simulation the code was run for several different values of negative ion concentration, initial temperatures, mass ratios and negative ion charge. The results in these simulations attest to the good efficiency and adequacy of the code for describing the free expansion process. In particular, the effects of mass and temperature separations are clearly exhibited. Moreover, it shows that the time-asymptotic solution is self-similar and that the plasma approaches the quasi-neutrality regime for long times. It is also found that the plasma temperature decreases as t^{-2} in the asymptotic regime.

The organization of the paper is as follows: in Section II we present the Vlasov–Poisson system used for describing the NIP expansion; in Section III we introduce the rescaling transformation for a three-component plasma; the numerical

results are presented in Section IV and the conclusions are discussed in Section V.

II. MATHEMATICAL MODEL

We consider a one-dimensional collisionless NIP freely expanding into vacuum and experiencing no external field. The unperturbed plasma densities are n_0, $(1-\varepsilon)n_0$ and εn_0 for, respectively, positive ions, electrons and negative ions.

The charge of the positive ions is $+e$ and the electrons and negative ions have charge $-e$. The basic Vlasov–Poisson system is

$$\frac{\partial f_e}{\partial t}+p\frac{\partial f_e}{\partial x}-E(x,t)\frac{\partial f_e}{\partial p}=0\,, \tag{1}$$

$$\frac{\partial f_i}{\partial t}+\frac{p}{M_{ie}}\frac{\partial f_i}{\partial x}+E(x,t)\frac{\partial f_i}{\partial p}=0\,, \tag{2}$$

$$\frac{\partial f_n}{\partial t}+\frac{p}{M_{ne}}\frac{\partial f_n}{\partial x}-E(x,t)\frac{\partial f_n}{\partial p}=0\,, \tag{3}$$

$$\frac{\partial E(x,t)}{\partial x}=\int_{-\infty}^{+\infty}[f_i-\varepsilon f_n-(1-\varepsilon)f_e]dp. \tag{4}$$

In Equations (1)–(4) the suffices e, i and n refer to electrons, positive ions and negative ions, respectively; M_{ie} is the quotient of the mass of the positive ions and electrons, $M_{ie}=m_i/m_e$; $M_{ne}=m_n/m_e$ is the quotient of the mass of the negative ions and electrons and $\varepsilon=n_{0\_}/n_0$ is the uniform negative ion concentration; the time is normalized by the inverse of the electron plasma frequency, $\omega_{pe}^{-1}=(4\pi n_0e^2/m_e)^{-1/2}$; the length by $\lambda_{De}=\sqrt{kT_e/4\pi n_0e^2}$, the electron Debye length; the momentum by $\sqrt{m_ekT_e}$; the densities by n_0 and the electric field by $m_e\omega_{pe}^2\lambda_{De}/e$.

Before attempting to analyze numerically Equations (1)–(4), we do some preliminary analytical work by introducing *rescaling transformations* in order to avoid the difficulties concerned with the free boundary conditions.

III. RESCALING WITH ''VARIABLE MASS''

Rescaling methods have been frequently used as an effective tool for obtaining solutions of nonlinear problems. Analytical and numerical applications of these methods can be found in the study of ordinary and partial differential equations.[11–13] The main goal of the rescaling technique is to introduce new space and time variables so that, asymptotically, the evolution of the system is totally absorbed by the rescaling. As a consequence, in the new variables the system is recast into a form where the physics becomes easier to interpret, at least for large times. Particularly, for the free expansion problem in the ''new space,'' the plasma experiences no expansion and the free boundary conditions are easily implemented; the plasma will then remain in a finite region of phase space.

Let us introduce new space, momentum and time variables, $(x,p,t)\mapsto(\xi,\Pi,\theta)$, as well as a rescaled electric field and distribution function as follows:

$$x=C(t)\xi, \tag{5}$$

$$dt=A(t)^2d\theta, \tag{6}$$

$$\Pi=[\mu(t)m]\eta,\quad \eta=\frac{d\xi}{d\theta},\quad \mu(t)=\frac{C^2(t)}{A^2(t)}, \tag{7}$$

$$E(x,t)=\tilde{E}(\xi,\theta), \tag{8}$$

$$f_s(x,p,t)=F_s(\xi,\Pi,\theta),\quad s=i,e,n. \tag{9}$$

The relation between the momentum $p=m_sv$ of the original phase space (x,p), and the new momentum Π is easily obtained from (5)–(7),

$$p=m_sv=\frac{\Pi}{C}+\xi\dot{C}m_s,\quad s=i,e,n, \tag{10}$$

which applies to all three species.

From (5) and (10) it can be easily verified that the Jacobian of this transformation is equal to unity independently of the choice of the arbitrary functions $A(t)$ and $C(t)$. Therefore a phase space element

$$dxdp=d\xi d\Pi, \tag{11}$$

is conserved and the choice (9) corresponds to the conservation of the number of particles,

$$f(x,p,t)dxdp=F(\xi,\Pi,\theta)d\xi d\Pi.$$

In reality the conservation of a phase space element is related to the fact that Eqs. (5)–(6) and (10) represent a canonical transformation which preserves the Hamiltonian formalism.[5,13]

In view of the transformation (5)–(10) we can write the Vlasov–Poisson system (1)–(4), in the space (ξ,Π), as follows:

$$\frac{\partial F_e}{\partial\theta}+\frac{\Pi A^2}{C^2}\frac{\partial F_e}{\partial\xi}-A^2C(\tilde{E}+\ddot{C}\xi)\frac{\partial F_e}{\partial\Pi}=0\,, \tag{12}$$

$$\frac{\partial F_i}{\partial\theta}+\frac{\Pi A^2}{M_{ie}C^2}\frac{\partial F_i}{\partial\xi}-A^2C(M_{ie}\ddot{C}\xi-\tilde{E})\frac{\partial F_i}{\partial\Pi}=0\,, \tag{13}$$

$$\frac{\partial F_n}{\partial\theta}+\frac{\Pi A^2}{M_{ne}C^2}\frac{\partial F_n}{\partial\xi}-A^2C(M_{ne}\ddot{C}\xi+\tilde{E})\frac{\partial F_n}{\partial\Pi}=0\,, \tag{14}$$

$$\frac{\partial\tilde{E}}{\partial\xi}=\int_{-\infty}^{+\infty}[F_i-(1-\varepsilon)F_e-\varepsilon F_n]d\Pi. \tag{15}$$

Although Equations (12)–(15) look rather complicated, we still have the freedom to choose the arbitrary functions $A(t)$ and $C(t)$, subject to the sole constraints of regularity and nonzero over $[0,\infty)$. In Ref. 5 it was shown that the functions $A(t)$ and $C(t)$ play different roles in the rescaling; $A(t)$ determines the time scale while $C(t)$ gives the structure of the phase space (ξ,Π). Therefore, $A(t)$ and $C(t)$ can be chosen independently. It is important to note, however, that no matter what time dependence we adopt for $A(t)$ and $C(t)$, this choice will not influence the solutions in the real phase space (x,p). In fact, their influence can be felt only in the rescaled space. Equations (12)–(15) can be interpretated as

describing a ''new'' physical system where the particles experience a modified interaction and the electric field $\tilde{E}$ obeys the Poisson law (15).

As an adequate choice for the functions $A(t)$ and $C(t)$ we take the same expansion law used in describing a two-component plasma expansion,

$$A^4 = C = 1 + \Omega t, \tag{16}$$

where Ω is an arbitrary frequency characterizing the transformation. With the values of $A(t)$ and $C(t)$ given by (16) the rescaled Vlasov–Poisson system for a NIP finally becomes

$$\frac{\partial F_e}{\partial \theta} + \frac{\Pi}{\mu(\theta)} \frac{\partial F_e}{\partial \xi} - \mu(\theta)\tilde{E}\frac{\partial F_e}{\partial \Pi} = 0\,, \tag{17}$$

$$\frac{\partial F_i}{\partial \theta} + \frac{\Pi}{M_{ie}\mu(\theta)} \frac{\partial F_i}{\partial \xi} + \mu(\theta)\tilde{E}\frac{\partial F_i}{\partial \Pi} = 0\,, \tag{18}$$

$$\frac{\partial F_n}{\partial \theta} + \frac{\Pi}{M_{ne}\mu(\theta)} \frac{\partial F_n}{\partial \xi} - \mu(\theta)\tilde{E}\frac{\partial F_n}{\partial \Pi} = 0\,, \tag{19}$$

$$\frac{\partial \tilde{E}}{\partial \xi} = \int_{-\infty}^{+\infty} [F_i - (1-\varepsilon)F_e - \varepsilon F_n]\, d\Pi, \tag{20}$$

where $\mu(\theta) = (1 + \Omega\theta/2)^3$. This is the system we shall use in our numerical analysis. The advantage in treating numerically Equations (17)–(20) rather than (1)–(4) is that the rescaled system describes the evolution of ''particles'' of variable mass $m_s\mu(\theta)$ which increases with time. As we shall show later this variable mass has the effect of bringing the particles to rest thus facilitating the application of the free boundary conditions.

IV. NUMERICAL RESULTS

The numerical analysis of the system (17)–(20) was performed with an Eulerian code, slightly modified to incorporate the time-dependent coefficients appearing in the Vlasov equations. Several simulation runs were done with different values of the parameters M_{ie}, M_{ne}, ε, Ω, negative ion charge and initial temperatures. The plots presented below show only that part of the phase space where $\xi > 0$ or $x > 0$. For $\xi < 0$ or $x < 0$, the results are symmetric. Space is measured in units of the electron Debye length, time in units of the inverse of the plasma frequency and velocity in units of the electron thermal velocity. For $t = 0$ the plasma is locally neutral having a uniform distribution from ξ or $x = -6$ to ξ or $x = 6$. In the velocity space the initial particle distribution is specified by the Maxwellian,

$$\exp(-m_s v^2/2T_s), \quad s = i, e, n,$$

where T_i, T_e and T_n are, respectively, the positive ion, electron and the negative ion temperatures. It is interesting to notice that here we keep both $C(t)$ and $A(t)$ at our disposal, while maintaining the invariance of the distribution function and of the phase volume element [Equations (9) and (11)]. In preceding works, mass was not allowed to change with time and we had to take $A = C$ (which indeed corresponds here to a constant mass). Then a choice $A < C$ brought in a positive friction, while now the same choice gives an increasing time mass. These are the true physical effects that bring the system to rest.

A. Phase space structures and thermodynamical properties

We begin by considering the following parameters values:

$$\Omega = 0.4,\ M_{ie} = 3,\ M_{ne} = 10,\ \varepsilon = 0.1,$$

$$T_e = 1,\ T_i = 0.5,\ T_n = 0.35.$$

The value of Ω is chosen empirically in such a way that during the simulation the plasma stays inside a finite region of the transformed space. Its optimum choice keeps the dimensions of the asymptotic state as close as possible to the dimensions of the initial state. The choice $\varepsilon = 0.1$ represents a mixture of negative species with 10% of negative ions and 90% of electrons. In all phase space graphs darker regions represent regions of higher density.

In Fig. 1 we show an example of the electron distribution function $F_e(\xi, \pi)$ in the transformed space (ξ, π). Notice that F_e develops a finer and finer structure in ξ, which leads to the loss of information on a local scale. The fundamental point in this simulation is that the rescaling transformation by confining the plasma on a finite interval, allows the preservation of the global information. This fact can be verified by performing the transformation back to the original (physical) space.

The complicated structure of Fig. 1 is unraveled by the back transformation into (x, v) space. The electron as well as the positive and negative ions distribution functions in real space (x, v) are shown in Figs. 2, 3 and 4, for several different time values. From these figures we can clearly see an evolution similar to that obtained for a two-component plasma expansion.[5] In the early stages some electrons run ahead the bulk of the plasma generating an electric field that accelerates a group of positive ions into vacuum. In the asymptotic regime, i.e., for large times the evolution becomes self-similar and the distribution functions assumes the form

$$f(x, v, t) = n(x, t)\,\delta(v - x/t).$$

This is indicated by the formation of a straight filamentary structure in phase space and corresponds to the asymptotic straight line trajectories determined by Luo and Yu (Fig. 2 of Ref. 8). It is interesting however to point that the same behavior is found here for the electrons and ions, besides the negative ions.

The net charge density in the rescaled space,

$$n(\xi) = \int [F_i(\xi, \Pi) - (1-\varepsilon)F_e(\xi, \Pi) - \varepsilon F_n(\xi, \Pi)]\, d\Pi,$$

is presented in Fig. 5. A formation of alternatively positive and negative layers is clearly seen in the early stages such as that presented in frame number two of Fig. 5. This indicates the effect of charge separation in the first stages of the expansion, where the less massive electrons lead the process, closely followed by the ions and only later by the more mas-

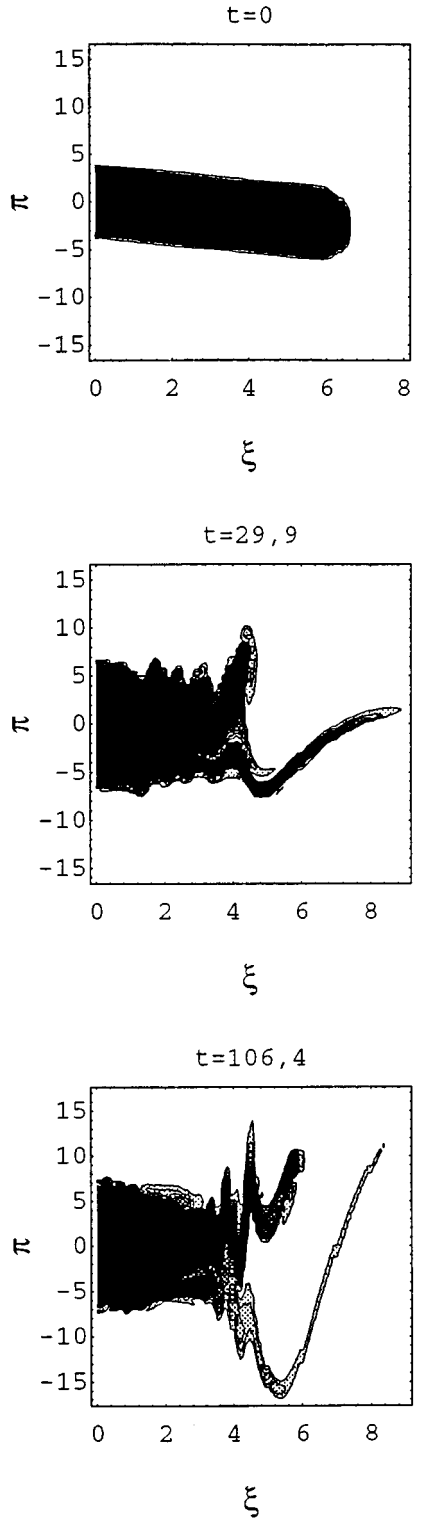

FIG. 1. Electron distribution function in rescaled phase space.

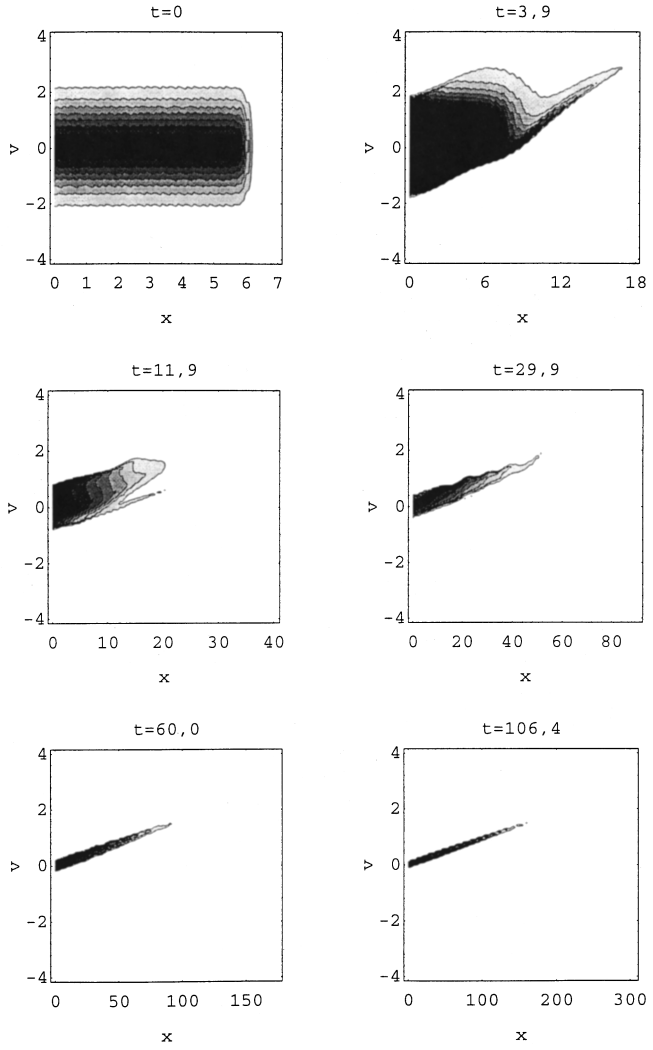

FIG. 2. Electron distribution function in real phase space.

sive negative ions. This layer formation will necessarily build an ambipolar field which tends to accelerate the negative ions as proposed in Ref. 9. Later we will show that, asymptotically the dimensions of these layers tend to zero faster than t in the rescaled space, assuring that the plasma becomes neutral over a smaller and smaller scale.

Figure 6 shows the negative ion density $n_n(\xi)$ (solid line), positive ion density $n_i(\xi)$ (broken line) and electron density $n_e(\xi)$ (dotted line) in the rescaled space. Again we can notice that charge neutrality is approached asymptotically. Nevertheless, this behavior differs slightly from that of an electron–ion plasma where the electron and ion densities tend to assume the same profile. In the case of a NIP the negative ions density vanishes before the plasma front, which is a consequence of their bigger inertia.

We now investigate some thermodynamical properties of the NIP expansion. Let us define the local temperature $T_s(x,t)$, pressure $P_s(x,t)$ and density $n_s(x,t)$ by

$$kT_s(x,t)=m\frac{\int(p-\langle p\rangle)^2 f_s(x,p,t)dp}{\int f_s(x,p,t)dp},$$

$$P_s(x,t)=m\int(p-\langle p\rangle)^2 f_s(x,p,t)dp, \quad s=i,e,n, \qquad (21)$$

$$n_s(x,t)=\int f_s(x,p,t)dp,$$

where k is the Boltzmann constant.

From the rescaling transformation given in Sec. III, we can define ''new'' temperature, pressure and density as

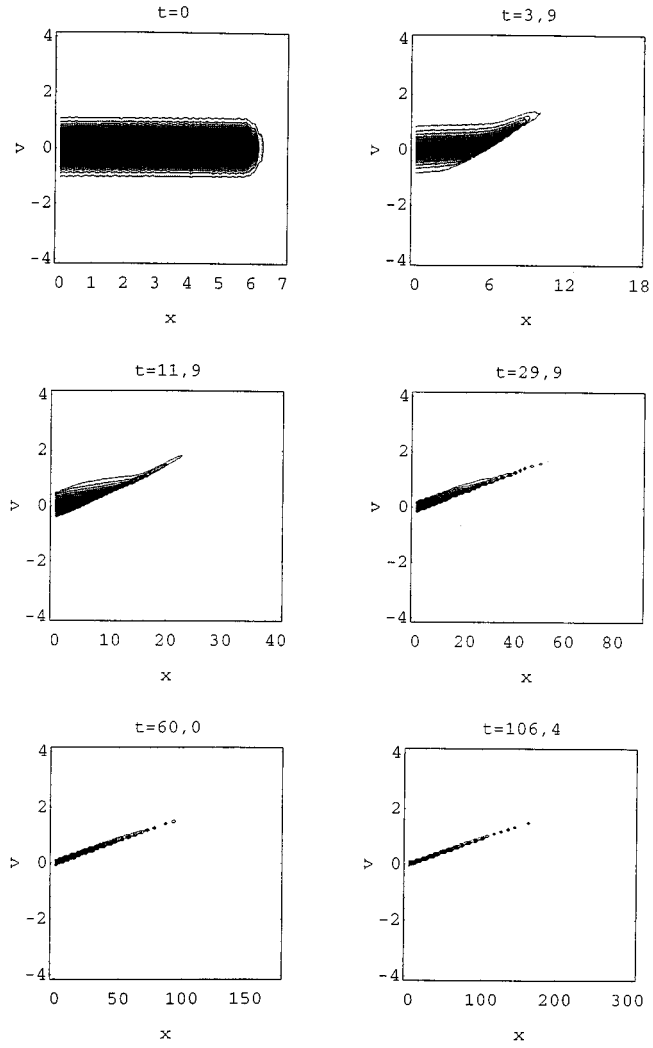

FIG. 3. Ion distribution function in real phase space.

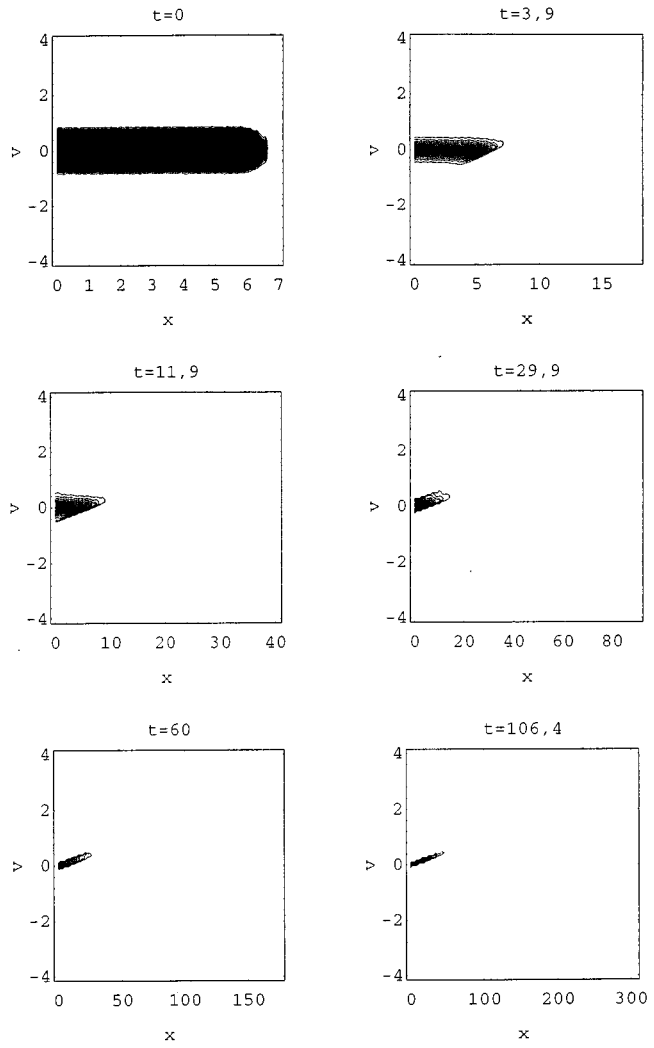

FIG. 4. Negative ion distribution function in real phase space.

$$k\hat{T}_s(\xi,\theta)=m\frac{\int(\Pi-\langle\Pi\rangle)^2F_s(\xi,\Pi,\theta)d\Pi}{\int F_s(\xi,\Pi,\theta)d\Pi},$$

$$\hat{P}_s(\xi,\theta)=m\int(\Pi-\langle\Pi\rangle)^2F_s(\xi,\Pi,\theta)d\Pi,\quad s=i,e,n, \tag{22}$$

$$\hat{n}_s(\xi,\theta)=\int F_s(\xi,\Pi,\theta)d\Pi.$$

The relations between the old [Equation (21)] and the new [Equation (22)] thermodynamical functions are given by

$$T_s(x,t)=[1/(1+\Omega t)^2]\hat{T}_s(\xi,\theta),$$

$$P_s(x,t)=[1/(1+\Omega t)^3]\hat{P}_s(\xi,\theta),\quad s=i,e,n, \tag{23}$$

$$n_s(x,t)=[1/(1+\Omega t)]\hat{n}_s(\xi,\theta).$$

The asymptotic behavior of the rescaled thermodynamical functions (22) indicates that the temperature evolution of the NIP is identical to that of a two-component plasma. This can be seen from Figs. 6 and 7, which show that, asymptotically, $\hat{P}_s$, $\hat{n}_s$ and $\hat{T}_s$ do not depend on time anymore ($\hat{T}_s$ is the ratio between $\hat{P}_s$ and $\hat{n}_s$). From Equation (23), it is easily seen that if $\hat{T}_s$ does not depend on time asymptotically then the temperature $T_s(x,t)$ decreases in time as t^{-2}.

We are now able to show that the dimensions of the charged layers (Fig. 5) tend to zero faster than t in the rescaled space. The Debye length is proportional to $(T/n)^{1/2}$, i.e.,

$$\lambda_D\sim(T/n)^{1/2}.$$

Since for large times the densities vary as t^{-1} and the temperatures as t^{-2}, then necessarily $\lambda_D\sim t^{-1/2}$. As a consequence, in the real space the Debye length tends to zero, indicating that the plasma goes into a regime of quasineutrality.

The potential and kinetic energies are presented in Fig. 8. This plot shows that the three kinetic energies are asymptotically constant. However, they oscillate differently, since the electrons, negative ions and positive ions have different masses. The potential energy is virtually zero and is multiplied by a factor of eight to allow it to be shown on the same scale as the kinetic energies.

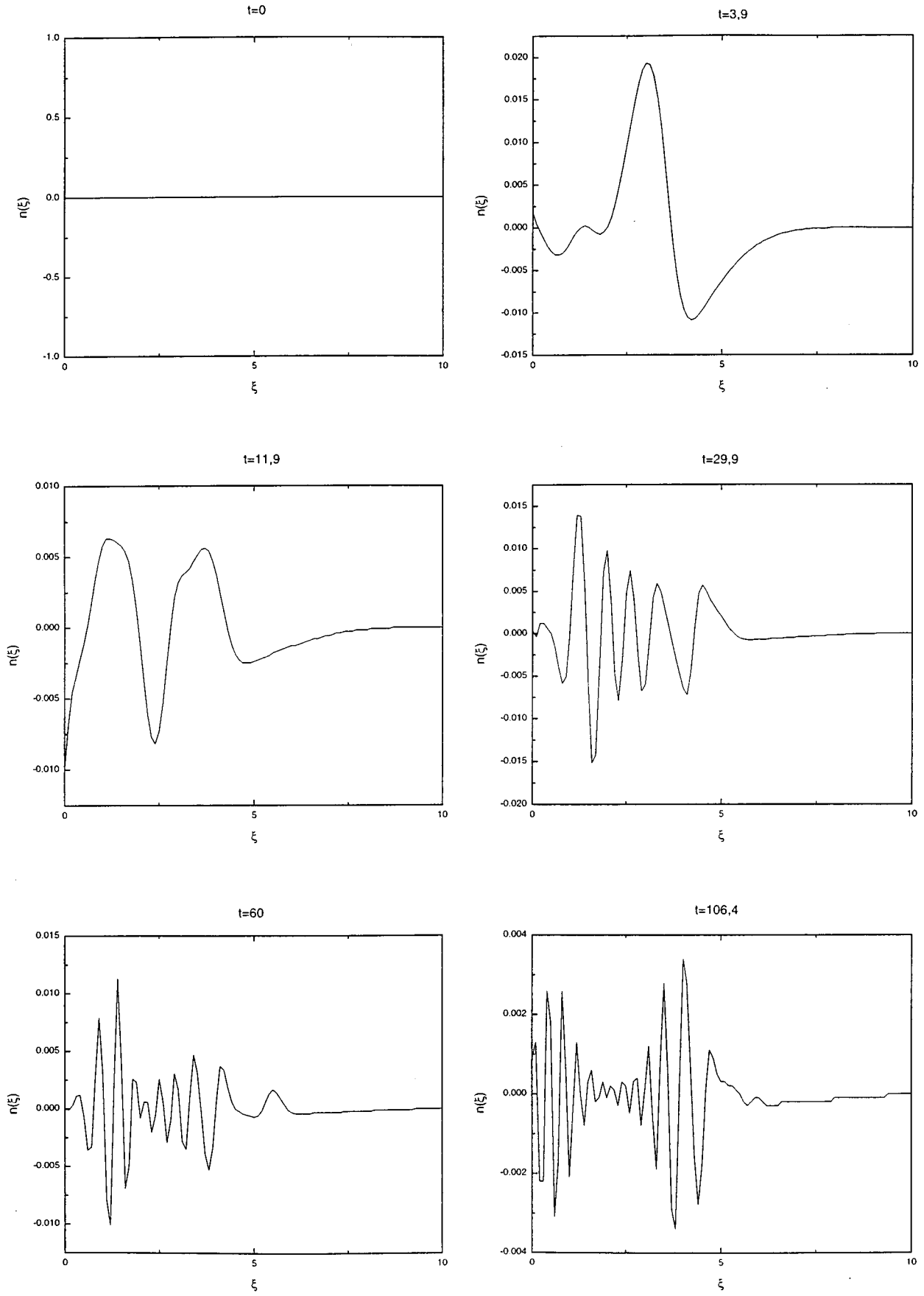

FIG. 5. Net charge density in rescaled space.

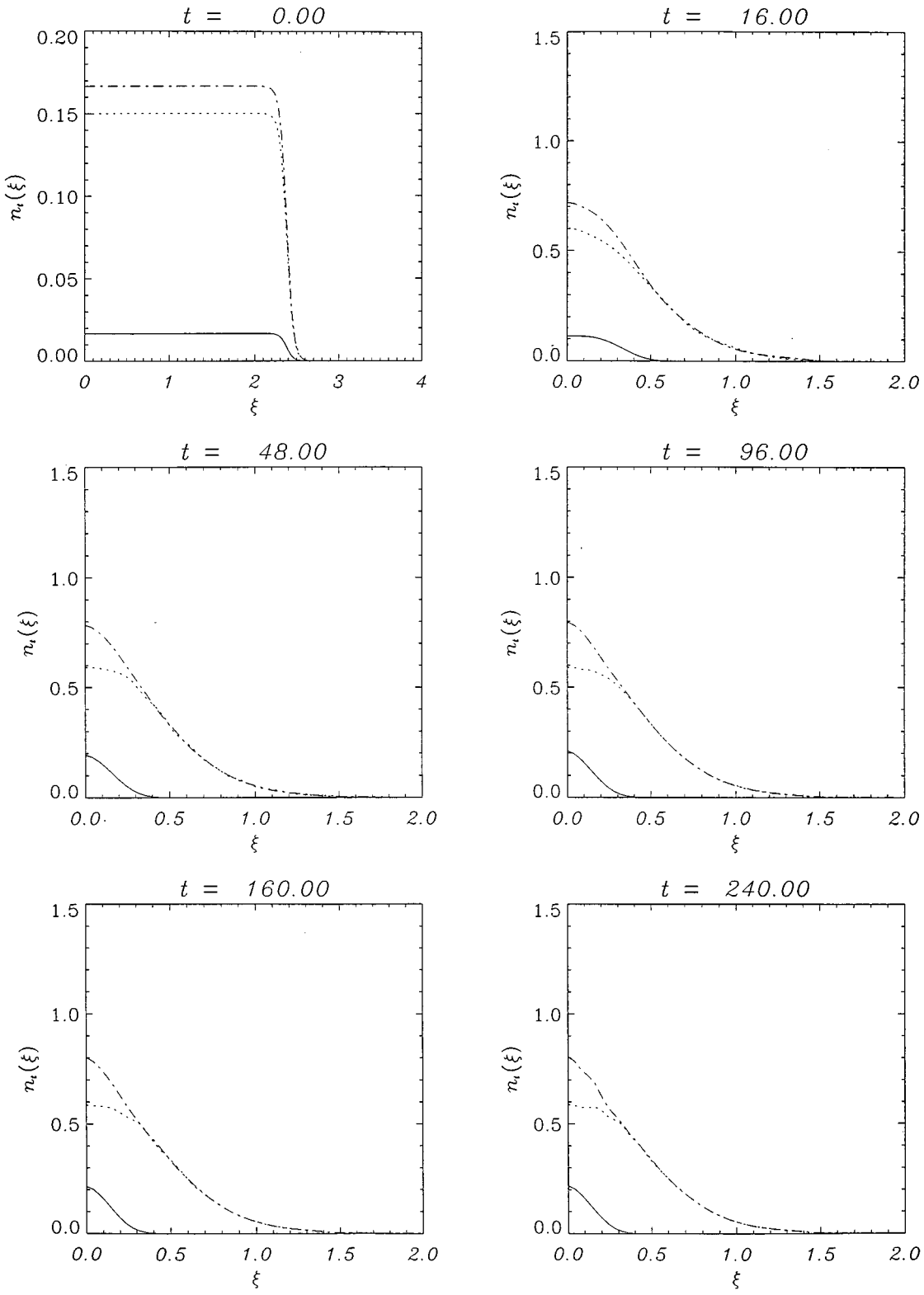

FIG. 6. Number density for electrons (dotted line), ions (broken line) and negative ions (solid line) in rescaled space for $\varepsilon = 0.1$.

B. Different mass ratios, initial temperatures and negative ions charge

It is interesting to study the evolution of each species under the variation of some of the parameters. In Fig. 9 the negative ions density, positive ions density and electrons density are shown in the rescaled space for a NIP with a mixture of 20% of negative ions and 80% of electrons. The effect of an additional increase in the negative ion concentration can be seen in Fig. 10. In this case the NIP contains the same number of electrons and negative ions ($\varepsilon = 0.5$). By comparing Figs. 6, 9 and 10, it can be seen that, as we increase the negative ions concentration, the electrons density

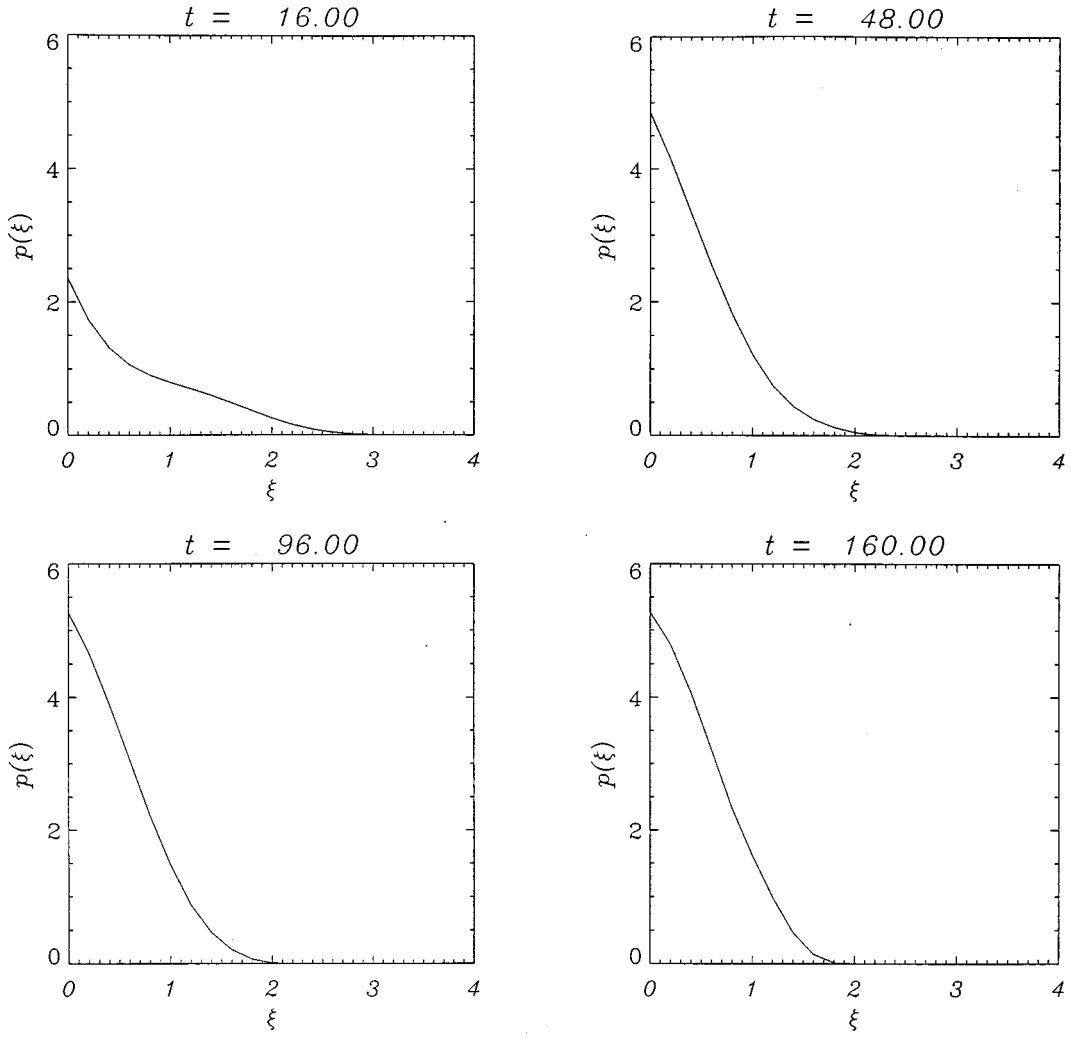

FIG. 7. Negative ion pressure in rescaled space.

starts to develop a hump. This corresponds to the fact that the rate at which the electrons leave the center of the plasma increases as we increase the proportion of negative ions.

Some other interesting features of the NIP expansion can be observed by using different values for initial temperatures, mass ratio and charge of negative ions. We checked the evolution of the three densities in the rescaled space for an NIP 50% of negative ions and 50% of electrons, but with temperatures $T_e = T_n = 1$, $T_i = 0.5$ and mass ratios $M_{ne} = 1$, $M_{ie} = 3$. In this case the negative ions are, in fact, electrons ($M_{ne} = 1$), starting with the same initial condition as the electrons. As expected, both species being equal behave exactly the same way. In Fig. 11 we present the results for the case when the negative ion temperature is set to the value $T_n = 0.5$. As expected on physical grounds, the cooler population stays behind and the hotter particles lead the expansion. Figure 12 shows the behavior of the expansion when we modify only the mass of the negative ions. Again, as expected on physical grounds, we can verify that the negative ions density goes to zero faster when their mass is increased. This implies a mass concentration effect as a consequence of the bigger inertia of the more massive negative ions.

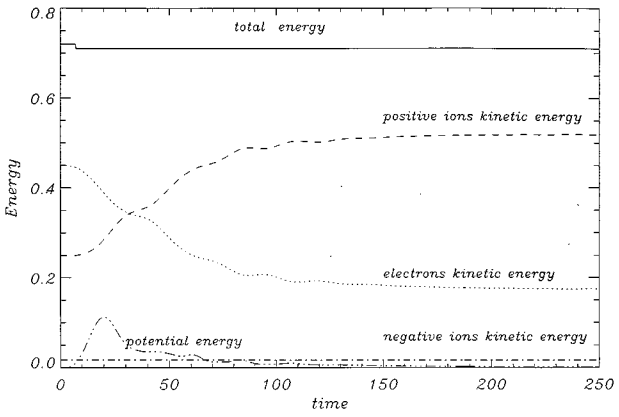

FIG. 8. Evolution of the kinetic and potential energies in time.

Another interesting point is to verify how the negative ions charge can affect the density profiles. To simulate the expansion of a NIP with different negative ions charge, we must modify Equations (3) and (4). Assuming that the negative ions charge is $-Ze$, we can replace (3) and (4) by

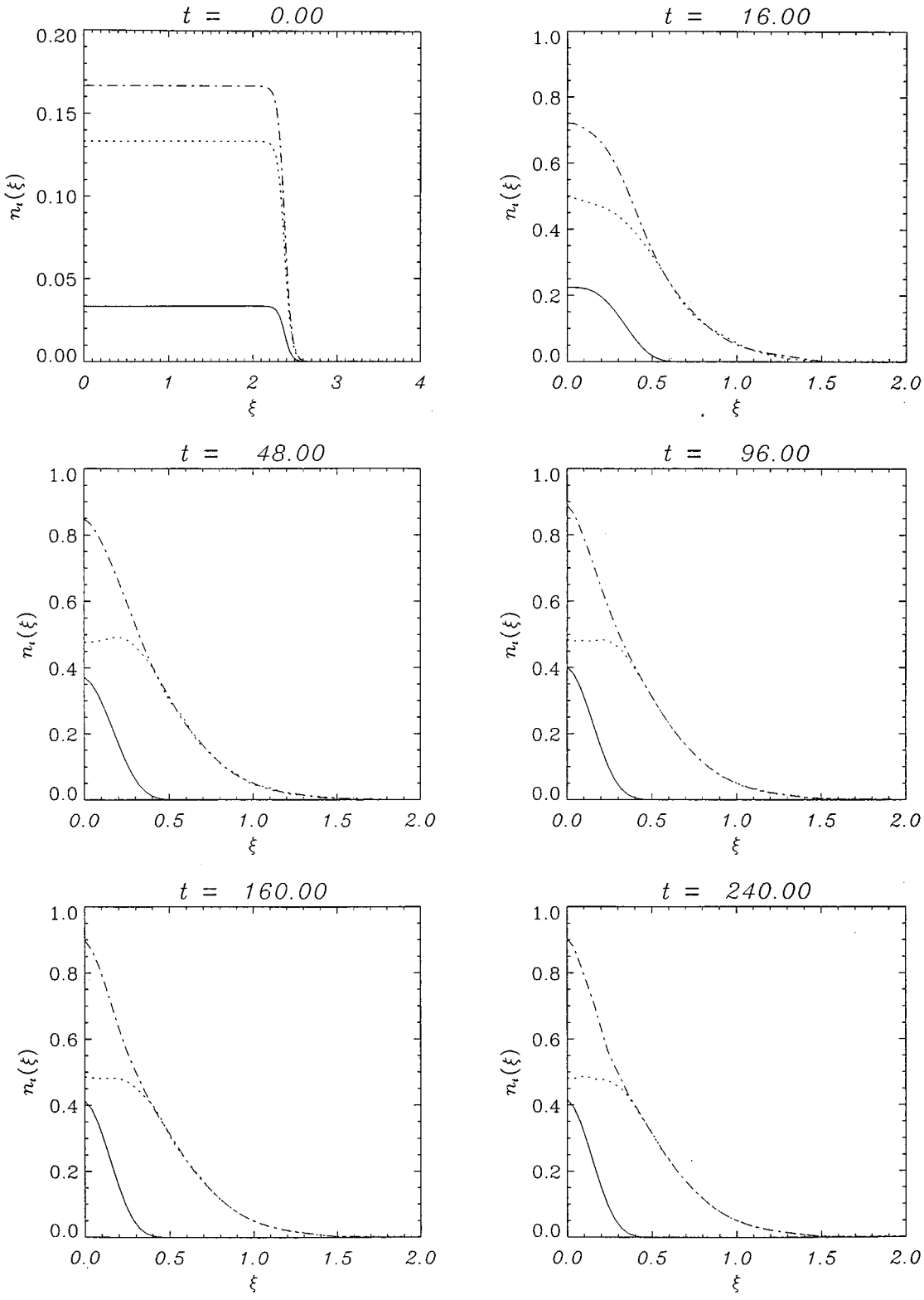

FIG. 9. Number density for electrons (dotted line), ions (broken line) and negative ions (solid line) in rescaled space for $\varepsilon = 0.2$.

$$\frac{\partial f_n}{\partial t} + \frac{p}{M_{ne}} \frac{\partial f_n}{\partial x} - ZE(x,t) \frac{\partial f_n}{\partial p} = 0 , \tag{24}$$

$$\frac{\partial E(x,t)}{\partial x} = \int_{-\infty}^{+\infty} [f_i - Z\varepsilon f_n - (1 - Z\varepsilon) f_e] dp, \tag{25}$$

respectively. The inclusion of the parameter Z in the dynamical equations represents no difficulties and the implementation in the numerical code is straightforward. In Fig. 13, we have used the same parameter values as in the referencial run ($T_e = T_n = 1$, $T_i = 0.5$, $M_{ne} = 1$ and $M_{ie} = 3$), except that

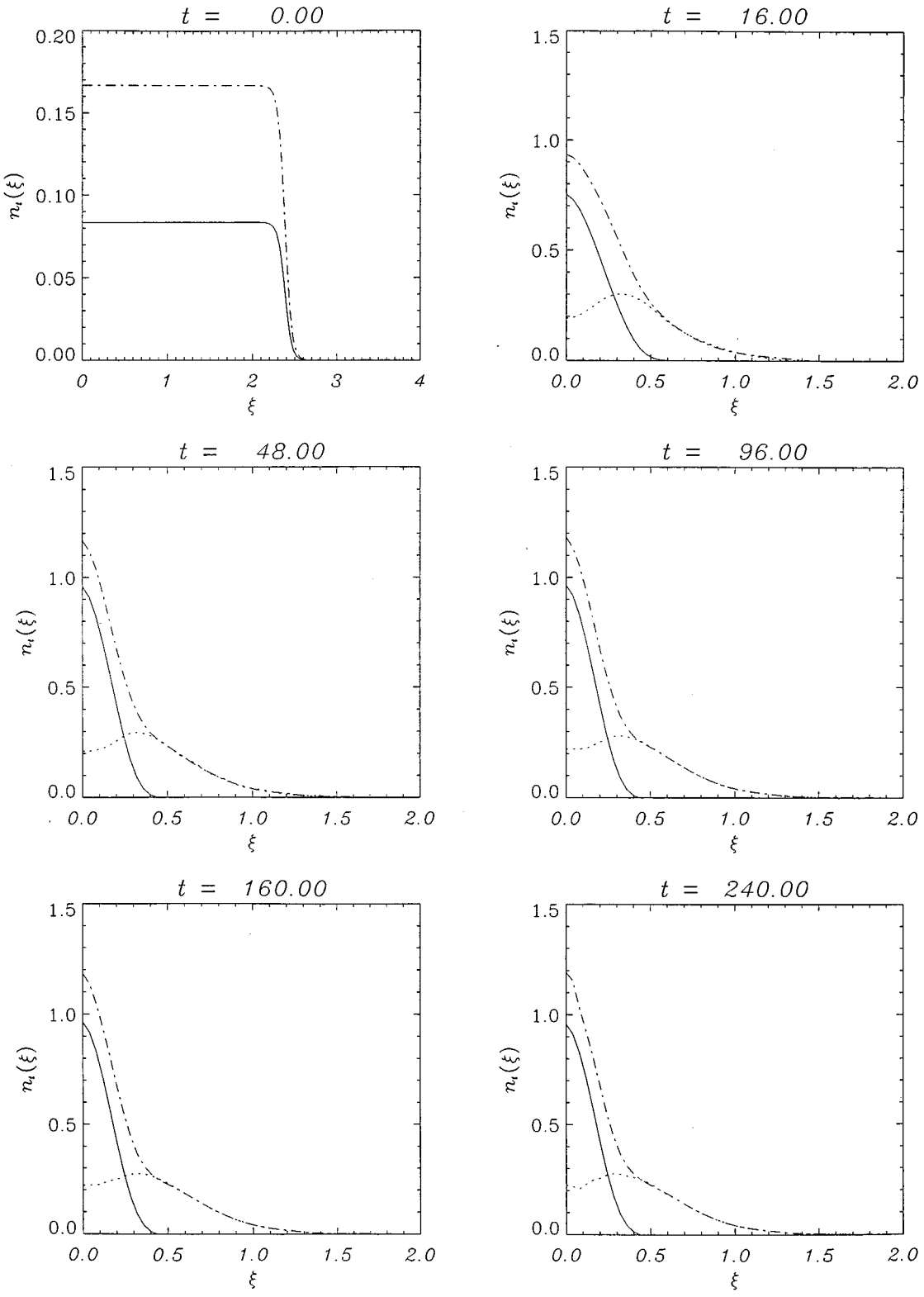

FIG. 10. Number density for electrons (dotted line), ions (broken line) and negative ions (solid line) in rescaled space for $\varepsilon = 0.5$.

$Z = 4$ and $\varepsilon = 0.125$. The densities of electrons and ions are kept the same as that of the referential run, but the density of negative ions is decreased in order to keep charge neutrality. The effect of increasing the negative ion charge can be seen in Fig. 13. Due to their larger charge, the negative ions tend to ''hold'' the positive ions and accelerate the electrons more effectively. In this sense it can be seen that, during the expansion ($t > 0$), the concentration of ions in the center of the plasma and of electrons in the front tend to increase (Fig. 13).

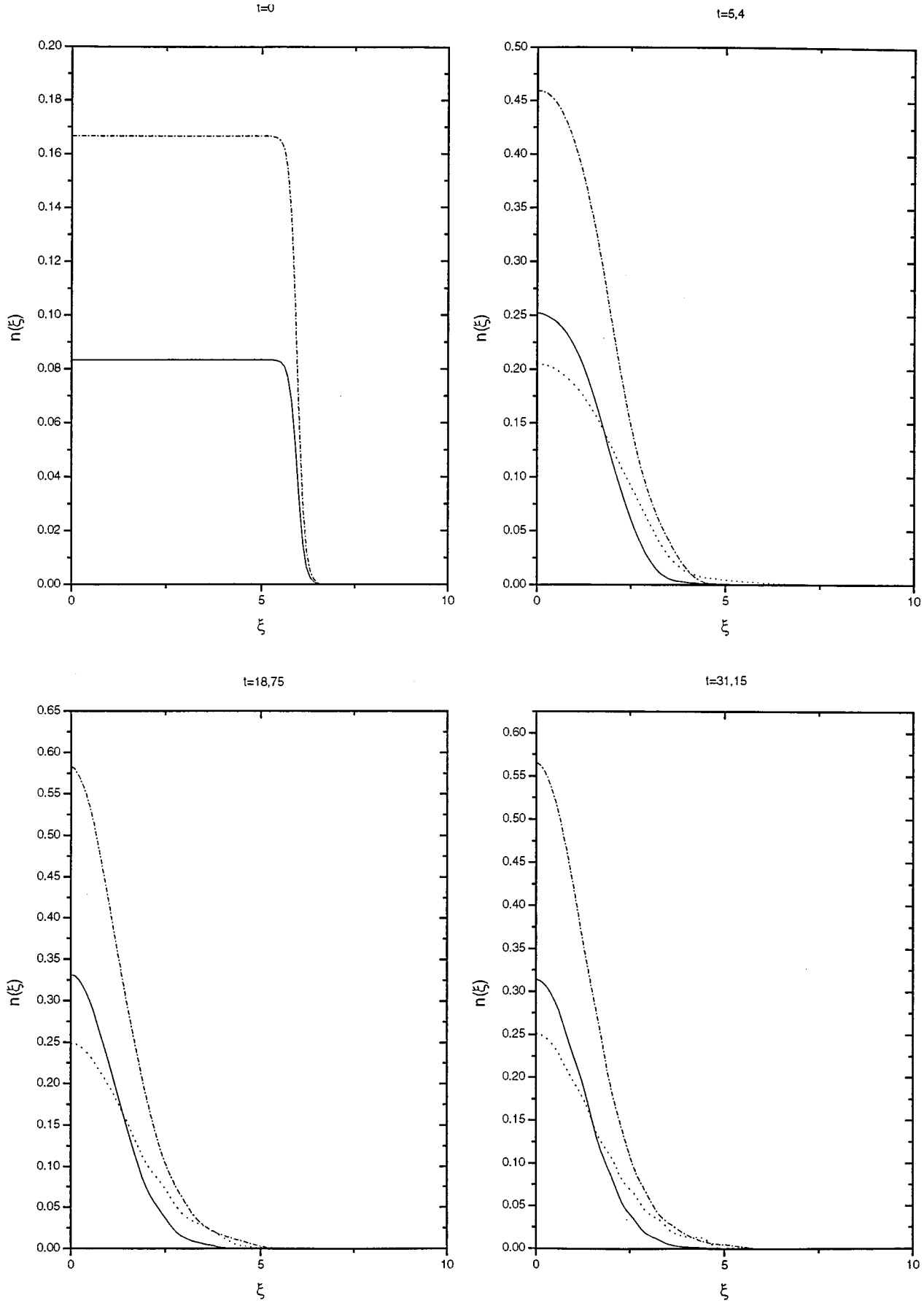

FIG. 11. Number density for electrons (dotted line), ions (broken line) and negative ions (solid line) in rescaled space; $T_e=1$, $T_i=0.5$, $T_n=0.5$, $M_{ne}=1$ and $M_{ie}=3$.

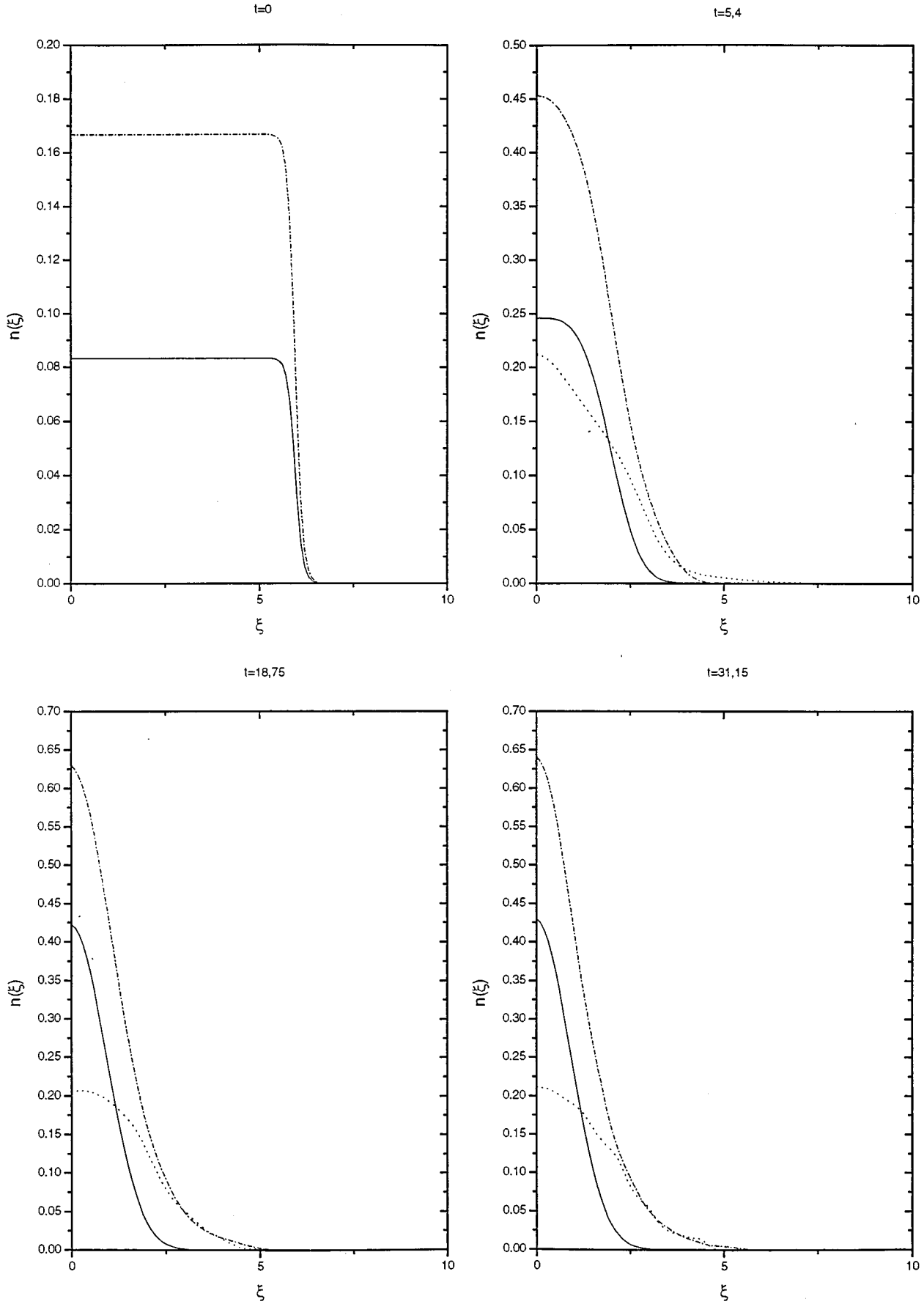

FIG. 12. Number density for electrons (dotted line), ions (broken line) and negative ions (solid line) in rescaled space; $T_e=1$, $T_i=0.5$, $T_n=1$, $M_{ne}=8$ and $M_{ie}=3$.

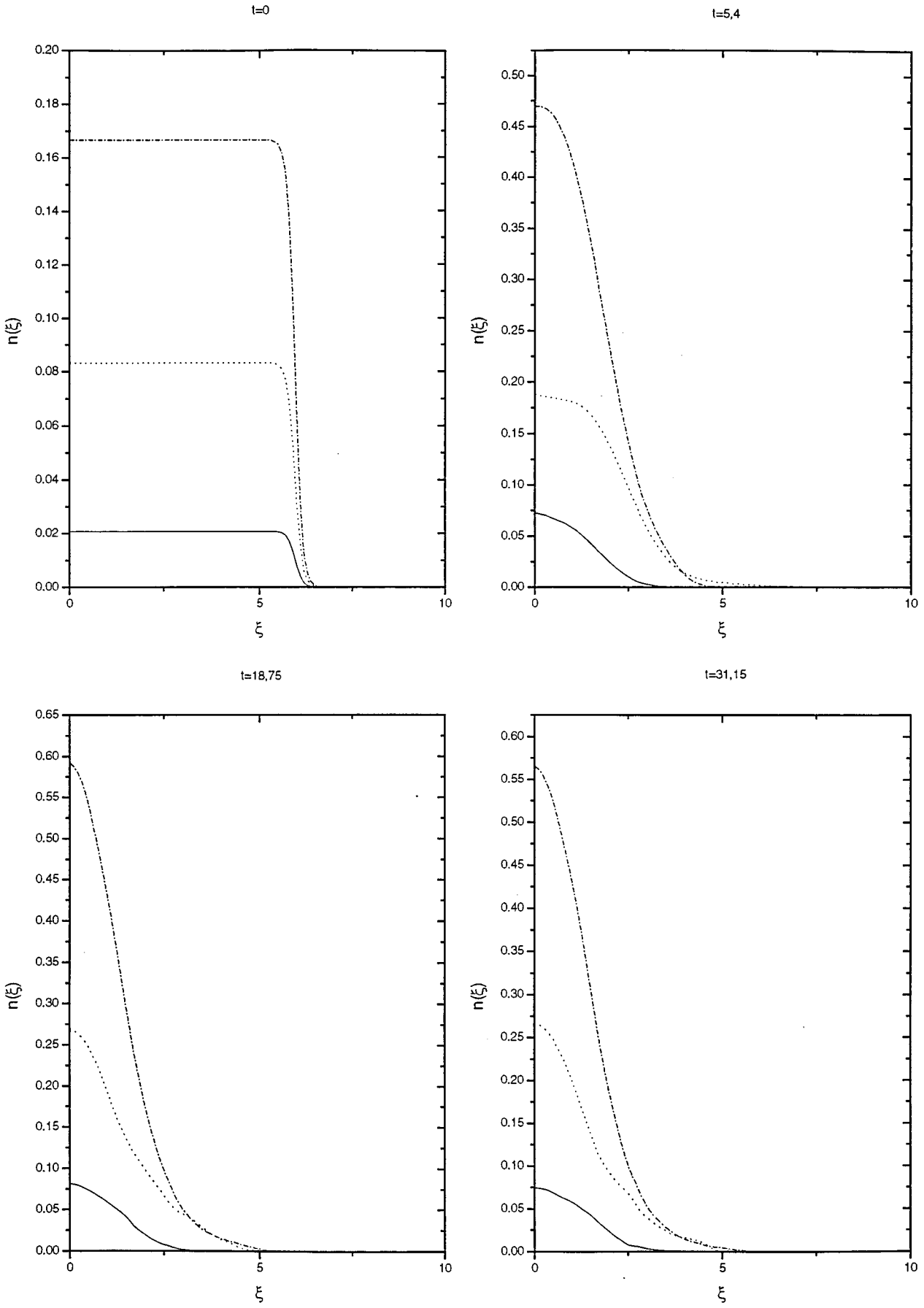

FIG. 13. Number density for electrons (dotted line), ions (broken line) and negative ions (solid line) in rescaled space; $T_e=1$, $T_i=0.5$, $T_n=1$, $M_{ne}=1$, $M_{ie}=3$, $Z=4$ and $\varepsilon=0.125$.

V. CONCLUSION

In this paper we analyzed numerically the process of free expansion into vacuum of a negative ion plasma. Paralleling the analysis of the expansion of the two-component plasma, a rescaling transformation of the basic equations was applied in order to deal with the moving boundary conditions. A splitting code for the Vlasov–Poisson equation was used to describe the dynamics of the expanding plasma. The Eulerian code allowed the treatment of the low density regime, a situation difficult to assess in a fluid or particle description. As expected on physical grounds, the numerical simulation accounted quite properly for the effects of mass and temperature segregation and for the existence of a time-asymptotic ballistic regime. The temperature follows the same t^{-2} power law as found in the two-component plasma study. These results attest to the adequacy and efficiency of the Eulerian code to treat the expansion process.

ACKNOWLEDGMENTS

We gratefully acknowledge G. Manfredi for fruitful discussions.

This work has been partially supported by the Brazilian agencies Conselho Nacional de Desenvolvimento Científico e Tecnológico (CNPq) and Financiadora de Estudos e Projetos (FINEP).

[1] A. V. Gurevich, L. V. Pariiskaya, and L. P. Pitaievskii, Sov. Phys. JETP **22**, 449 (1966).
[2] A. V. Gurevich, L. P. Pitoevskii, and V. V. Smirnova, Space Sci. Rev. **9**, 805 (1969).
[3] P. Wagli and T. P. Donaldson, Phys. Rev. Lett. **40**, 875 (1978).
[4] J. S. Pearlman, J. J. Thomson, and C. E. Max, Phys. Rev. Lett. **38**, 1397 (1977).
[5] G. Manfredi, S. Mola, and M. R. Feix, Phys. Fluids B **5**, 388 (1993).
[6] Y. El-Zein, A. Amin, H.-S. Kim, S. Yi, and K. E. Lonngren, Phys. Plasmas **2**, 1073 (1995).
[7] H. Luo and M. Y. Yu, Phys. Fluids B **4**, 3066 (1992).
[8] H. Luo and M. Y. Yu, Phys. Fluids B **4**, 1122 (1992).
[9] M. Y. Yu and H. Luo, Phys. Lett. A **161**, 506 (1992).
[10] M. Y. Yu and H. Luo, Phys. Plasmas **2**, 591 (1995).
[11] J. R. Burgan, M. R. Feix, E. Fijalkow, and A. Munier, J. Plasma Phys. **29**, 139 (1983).
[12] D. Besnard, J. R. Burgan, M. R. Feix, E. Fijalkow, and A. Munier, J. Math. Phys. **5**, 1123 (1983).
[13] S. Mola, G. Manfredi, and M. R. Feix, J. Plasma Phys. **50**, 145 (1993).